Shape memory characteristics of injection molded, cross-linked all-polyethylene composites

Tatár B., Tóth E., Molnár K., Mészáros L.

Radiation Physics and Chemistry 226 (2025) 112290

Contents lists available at ScienceDirect

Radiation Physics and Chemistry

journal homepage: www.elsevier.com/locate/radphyschem

Shape memory characteristics of injection molded, cross-linked all-polyethylene composites

Balázs Tatár [a], Eszter Tóth [a], Kolos Molnár [a,b,c,*], László Mészáros [a,b,**]

[a] Department of Polymer Engineering, Faculty of Mechanical Engineering, Budapest University of Technology and Economics, Műegyetem rkp. 3., H-1111, Budapest, Hungary
[b] HUN-REN Research Group for Composite Science and Technology, H-1111, Műegyetem rkp. 3., H-1111, Budapest, Hungary
[c] MTA-BME Lendület Sustainable Polymers Research Group, Műegyetem rkp. 3, H-1111, Budapest, Hungary

ARTICLE INFO

Handling Editor: Piotr Ulanski

Keywords:
Polymer-matrix composites (PMCs)
Polymer fibers
Shape memory behavior
Injection molding
Gamma irradiation

ABSTRACT

In this study, we investigated the shape memory properties of a novel self-reinforced polymer composite (SRPC). Chopped Dyneema® SK76 fibers were mixed with high-density polyethylene (HDPE) resin, and samples were produced by injection molding. To allow the fibers to keep their shape and reinforce effectively, we cross-linked them with gamma irradiation (100, 200, and 300 kGy absorbed doses). In the second step of irradiation, we irradiated the composites with doses of 50, 100, 150, and 200 kGy to give them shape memory properties. Soxhlet extractions, differential scanning calorimetry, and scanning electron microscopy revealed that the fibers cross-linked and kept their structural integrity through processing. We confirmed the reinforcing effect of the fibers with flexural tests and by dynamic mechanical analysis. In free recovery experiments, samples had recovery and fixity ratios above 79%. With the highest dose, recovery stress increased by 26%. We showed the viability of this novel method of self-reinforcement in the production of shape memory polymers (SMPs) with improved characteristics.

1. Introduction

Shape memory polymers (SMPs) are increasingly getting into the focus of research on shape memory materials, a class of intelligent materials that are capable of altering their shape in response to an external non-mechanical stimulus. SMPs are lightweight and can store energy and recover their shape even after great deformation. In addition, they can be engineered to respond to various stimuli, like heat, electricity, pH, moisture, light, etc. (Bhanushali et al., 2022; Zhang, 2022).

The shape memory effect in polymers relies on a dual structure, where the polymer must possess so-called switches and netpoints, both of which can be bonds or phases. Switches enable or disable the deformability of the material, depending on a stimulus, while netpoints remain in place throughout, keeping the material's integrity (Behl et al., 2010). One of the most common shape memory polymers is cross-linked polyethylene (X-PE). This material, in general, is used as tubes in plumbing, hoses, ducts, and housings in the automotive sector and artificial joints where shape memory has no role (Peacock, 2000). On the other hand, X-PE is a widely used heat-shrink tubing where good electric insulation is coupled with the shape memory effect (Jyotishkumar et al., 2019).

In X-PE, cross-links act as the netpoints, and the crystalline phase fills the role of the switches. X-PE is capable of shape memory in response to a heat stimulus. At the crystal melting temperature (T_m), the chains unfold within the crystalline domains. On the other hand, the cross-linked amorphous phase cannot be melted, therefore even though the crystalline phase turns amorphous above T_m, the material remains solid. T_m can be used as the switching temperature: this is where we need to heat up the pre-programmed shrink tubing to trigger its shape memory effect (Xia et al., 2021; Ota, 1981).

For X-PE, a shape memory cycle involves the following steps: first, the SMP is heated above its transition temperature (T_m), causing the switches (crystalline phase domains) to release as a result of melting. At this temperature, the netpoints, the cross-links between molecules, keep

* Corresponding author. Department of Polymer Engineering, Faculty of Mechanical Engineering, Budapest University of Technology and Economics, Műegyetem rkp. 3., H-1111, Budapest, Hungary.
** Corresponding author. Department of Polymer Engineering, Faculty of Mechanical Engineering, Budapest University of Technology and Economics, Műegyetem rkp. 3., H-1111, Budapest, Hungary.
E-mail addresses: molnar@pt.bme.hu (K. Molnár), meszaros.laszlo@gpk.bme.hu (L. Mészáros).

https://doi.org/10.1016/j.radphyschem.2024.112290
Received 3 May 2024; Received in revised form 6 September 2024; Accepted 13 October 2024
Available online 16 October 2024

the material in a solid state in which the material is easy to deform. The material can be converted into its programmed shape. Then, it needs to be cooled down below the crystallization temperature (T_c), which is below T_m, so that the switches can lock via forming new crystalline domains. During this process, some of the internal energy resulting from the deformation gets stored within the netpoints. Subsequently, when the switches are released again by the temperature stimulus, this stored energy enables the SMP to return to its original shape (Behl et al., 2010; Ota, 1981). The more energy we can store, the higher the forces during shape recovery. And that is the typical bottleneck of SMPs: their recovery stress is very small compared to metals (Behl et al., 2010).

With SMPs, high levels of deformation can be memorized, but shape recovery is never perfect. These factors are commonly assessed with the shape fixity ratio (R_f) and the shape recovery ratio (R_r), as described in Equations (1) and (2).

$$R_f = \frac{\varepsilon_u}{\varepsilon_m}\ [-], \tag{1}$$

$$R_r = \frac{\varepsilon_m - \varepsilon_p}{\varepsilon_m}\ [-], \tag{2}$$

where ε_m is the maximum strain applied, ε_u is the strain after unloading, and ε_p is the persisting strain after recovery (Jeewantha et al., 2022).

One area of research where the shape memory of polyethylene (PE) fibers is utilized is artificial muscles, where the high strength and shape memory of ultra-high molecular weight polyethylene (UHMWPE) fibers are exploited (Li et al., 2022; Maksimkin et al., 2018, 2019). Maksimkin et al. (2014) examined the shape memory behavior of UHMWPE fibers. Although the polymer lacks chemical cross-links, its high molecular weight allows the entanglement of amorphous chains to act as the netpoints, while the crystalline domains can act as the switches. The researchers compared these findings with UHMWPE in its bulk state, which also displayed shape memory due to similar mechanisms. Notably, UHMWPE fibers exhibited significantly greater recovery stress when compared to the bulk samples.

Reinforcement by fibers and nanoparticles is widely recognized as a highly effective method of enhancing the recovery stress (σ_{rec}) of SMPs (Jyotishkumar et al., 2019; Fejos et al., 2012; Rahman et al., 2017; Liu et al., 2018; Li et al., 2019). For this reason and others, the shape memory of X-PE composites has also been investigated. Wang et al., 2014a, 2014b explored the effects of short glass fibers on cross-linked poly (styrene-b-butadiene-b-styrene) (SBS) triblock copolymer/X-PE blends. They discovered that the inclusion of glass fibers resulted in a decelerated recovery process. However, repeated recovery tests demonstrated an increase in R_r for these blends. Wang et al. also investigated (Wang et al., 2016) carbon fiber reinforcement. It also led to slower recovery but increased the fixity ratio (R_f). Interestingly, with higher carbon fiber content, there was a decrease in the recovery ratio (R_r). Rezanejad and Kokabi (2007) added nanoclay particles to the X-PE matrix. The presence of nanoclay resulted in increased σ_{rec} while R_r and elongation at break decreased. Reinforcement increases σ_{rec} but decreases deformability and the precision of recovery.

A special type of reinforcement is self-reinforcement but so far, its effect on shape memory characteristics has been little researched. In self-reinforced polymer composites (SRPCs) or single-polymer composites, both the reinforcing structure and the embedding matrix are composed of the same family of polymers. Consequently, in SRPCs, the adhesion between the matrix and the reinforcement is excellent, which results in good resistance to crack propagation (Kmetty et al., 2010). Self-reinforcement offers a still unexplored but promising approach to enhancing material properties and recovery stress while keeping density low, deformability high, and the shape recovery ratio high.

Studies on self-reinforcement often focus on polypropylene (PP) (Kmetty et al., 2012, 2013; Vadas et al., 2018; Kara and Molnar, 2022) or polyethylene (PE) (Amer and Ganapathiraju, 2001; Hine et al., 2000, 2008). From the point of view of shape memory, PE is more interesting because, unlike PP, it can be relatively easily cross-linked, which greatly improves its shape memory effect. In PE, cross-linking involves breaking a hydrogen atom away from the polymer backbone, resulting in the formation of a reactive free radical. This radical can then combine with another free radical on a nearby chain, leading to the formation of a cross-link. Cross-linking is commonly achieved either by mixing a peroxide into the polymer melt or by applying high-energy ionizing radiation. The benefit of ionizing radiation is that it does not require any reactive and toxic additives and that cross-linking can be carried out on the finished product as a post-processing step. In PE, ionizing radiation creates most cross-links in the amorphous phase, resulting in a polymer that is both cross-linked and semi-crystalline. Since the long polymer chains pass through both the amorphous and the crystalline phase, according to the fringed micelle model or the switchboard model, the cross-linking affects the entire material, making it unable to melt or dissolve. Several types of irradiation can have an ionizing effect, such as electron irradiation or gamma irradiation. Their effects on the polymer are identical, but gamma irradiation is a slower process, which can penetrate deeper into the material, producing free radicals randomly in the entire cross-section (Peacock, 2000).

Many researchers have investigated PE composites reinforced with high-performance polyethylene (HPPE) fibers (Amer and Ganapathiraju, 2001; Hine et al., 2000, 2008). These fibers are made of ultra-high molecular weight polyethylene (UHMWPE), an exceptional type of PE that is widely used in medical implants (Nemes-Károly and Szebényi, 2023). These composites can be processed typically by film-stacking and hot compaction. These methods apply moderate temperatures and gentle shear forces to minimize damage to the fibers. On the other hand, these methods only allow the production of shell-like components with a long cycle time. Notably, these production methods are usually not productive and very restrictive in the geometries they allow (Kmetty et al., 2010). The typical fiber contents for these composites range from 20% to 70%. The reinforcement can increase the modulus and tensile strength by 200–300% and even more in some cases (Amer and Ganapathiraju, 2001; Hine et al., 2000, 2008).

Other processing methods are more productive, such as specialized injection molding. However, with these methods, cycle times become longer or the complexity of the parts decreases. Wang et al. (2022) produced SRPCs by injection molding via laying an HPPE fabric insert into the mold and injecting the matrix material onto it, raising tensile strength to 7.6 times the strength of the reference. Huang et al., 2014a, 2014b blended ultra-low molecular weight polyethylene with UHMWPE, both irradiated and unirradiated, and used shear-controlled orientation in injection molding to make SRPCs. With irradiation, they achieved better results. Wear rate and fatigue resistance increased, as did tensile strength and tensile modulus, the former by 192% and the latter by 58.4% compared to neat UHMWPE.

However, the shape memory properties of SRPCs are yet to be investigated. It is likely that self-reinforcement can effectively raise σ_{rec} as it is often correlated with the material's strength, as shown for UHWMPE fibers as well (Maksimkin et al., 2014). Such composites can combine the advantages of SRPC, such as low density and good adhesion, with superior shape memory properties (Kmetty et al., 2010).

In a previous study, we showed that by cross-linking the HPPE reinforcing fibers, conventional injection molding can also be used to manufacture SRPCs. We cross-linked PE fibers so they would not melt throughout the injection molding process. The irradiated fibers were compounded with the HDPE matrix and then injection molded. The matrix ensures the proper flow of the material, while the cross-linked fibers must keep their structural integrity to reinforce effectively (Mészáros et al., 2022). The higher strength of the composite indicates that the shape recovery stress can also be increased. (Tatár and Mészáros, 2024).

In this study, we produced polyethylene SRPCs with this novel technique and applied a further irradiation step to give them shape memory properties. Our hypothesis is that their effective reinforcement

can, much like other fiber reinforcement, increase the recovery stress of the SMP matrix. We then studied the structural, mechanical, crystalline, and shape memory properties of the composites in detail to determine and explain the effect of fibers on shape memory and recovery stress.

2. Materials and methods

2.1. Materials

For SRPCs, we chose an HDPE material as the matrix, Tipelin BA 550-13 (MOLGroup Chemicals, Hungary). It has a tensile stress at yield of 29 MPa and a flexural modulus of 1.5 GPa. This grade is recommended for blow molding, but it is also suitable for injection molding.

We used Dyneema® SK76 HPPE fibers (Koninklijke DSM N. V., Netherlands) as reinforcement. These fibers have a diameter of 12–21 μm, high strength (3.3–3.9 GPa), and high modulus (109–132 GPa), according to Dyneema's fact sheet, thus they are well-suited for their role as fiber reinforcement.

2.2. Production of shape memory materials

First, the fiber strands were manually chopped into approx. 10–12 mm long pieces. These were sealed in PE bags and gamma-irradiated with doses of 100, 200, and 300 kGy. Izotóp Intézet Kft. (Budapest, Hungary) conducted the irradiation with a panoramic SLL-01 ^{60}Co radiation source, with a steady irradiation rate of 2 kGy/h. Our previous experiments showed these doses to be sufficient for cross-linking (Meszaros et al., 2022). High doses were selected, as the cross-linking takes place mainly in the amorphous phase, making it more difficult to cross-link the fibers with high degrees of crystallinity (Zhang et al., 2023). Some of the samples were kept as reference (0 kGy dose).

As a compromise between good mechanical properties and few complications during compounding, we chose a fiber content of 20 wt%. The irradiated chopped fibers and the matrix were mixed in a Labtech LTE 26–44 twin-screw extruder (Labtech Engineering Co., Ltd., Thailand) at 190 °C. A double-hole filament die was used at 190 °C. The extruded filaments were cooled with air and then pelletized with a Labtech LZ-120/VS pelletizer (Labtech Engineering Co., Ltd., Thailand). Four types of pellets were produced, each containing fibers irradiated with doses of 0, 100, 200, or 300 kGy. Even though the virgin HPPE fibers have a higher melting point (142–147 °C) than that of HDPE, they melt during compounding at 190 °C. The reference (0 kGy), therefore, can be considered a blend of the two PE grades.

The pellets containing the irradiated fibers were subsequently fed into an Arburg Allrounder 420C injection molding machine (Arburg GmbH, Germany). We injection molded standard 1A type dumbbell specimens with a cross-section of 4 × 10 mm, following the ISO 527 standard. Additionally, specimens were also injection molded from neat HDPE resin as reference. The composites required processing at 200 °C for complete cavity filling. Injection rate was 55 cm^3/s, injection pressure was 2000 bar and holding pressure was 1500 bar.

We needed the shape memory effect from not only the fibers but also the composites. Therefore, we also subjected the injection molded composite and neat specimens to gamma irradiation with the above-mentioned device. The doses were 50, 100, 150, and 200 kGy. We also kept a reference (0 kGy).

Thus, we created composite samples with fibers of 4 different absorbed doses (0, 100, 200, and 300 kGy) and irradiated these composites with four different doses (50, 100, 150, and 200 kGy). We also had references without a second irradiation step and samples with no fibers.

We named the samples *PxFy*, where *x* is the dose absorbed during post-processing, and *y* is the dose absorbed by the fibers (preceding composite preparation), with "*PxRef*" being the sample with no fibers and „*PxF0*" being the sample with the unirradiated fibers. Note that fibers were irradiated twice; for instance, P100F200 means that the sample adsorbed 100 kGy dose during post-processing, while the fibers were treated with a 200 kGy dose in advance. Thus, the total adsorbed dose of fibers is the sum of the two numbers, 300 kGy in this case.

2.3. Characterization methods

2.3.1. Flexural test

We conducted 3-point bending tests on the specimens. We tested five specimens of each type on a Zwick Z005 universal testing machine (Zwick GmbH., Germany). The test speed was 10 mm/s, and the support span was 64 mm. The tests lasted until the specimen reached the conventional deflection, 10% of the span length (6.4 mm). We calculated the flexural modulus as the slope of the tangent at the initial straight part of the bending curve.

2.3.2. Soxhlet extraction

We used an *R 256 S* Soxhlet extractor manufactured by BEHR Labor Technik GmbH (Germany) to determine the effectiveness of cross-linking through the calculation of the gel fraction of the samples, where an increase in gel fraction would indicate cross-linking. We examined both irradiated and non-irradiated SRPC samples. We cut and weighed approximately 1 g of the samples, then put them in cellulose sample holder capsules and placed them in the extractor at random positions. For the extraction, we employed a boiling mixture of xylene isomers (boiling point: 139.3 °C) as the solvent and carried out the extraction for 24 h. The gel fraction was subsequently determined by dividing the initial mass by the remaining mass after extraction.

2.3.3. Scanning electron microscopy (SEM)

After Soxhlet extraction, we investigated the material residues using a JEOL JSM 6380LA (Jeol Ltd., Japan) scanning electron microscope (SEM). Before inspecting the samples, they were sputtered with a thin layer of gold. Using the test, we wished to see the effect of irradiation on the microstructure of samples.

2.3.4. Differential scanning calorimetry (DSC)

We investigated the crystalline properties of the samples using a TA Instruments Q2000 differential scanning calorimeter (DSC; TA Instruments, USA). We wanted to see how fibers and irradiation influence the crystal melting properties and determine the temperature range suitable for shape memory tests.

We cut and weighed 5–7 mg samples and investigated them between 40 and 210 °C in a heat-cool-heat cycle. The heating and cooling rate was 5 °C/min 293 J/g was used for the crystalline melting enthalpy of 100% crystalline PE (Wunderlich, 2012).

2.3.5. Dynamic mechanical analysis (DMA)

We also tested the samples by DMA in a TA Instruments Q800 device (TA Instruments, USA). The DMA tests tie together the mechanical and thermal properties. While the properties of the material at room temperature are the most important, the trends observed there may not hold at the temperatures of the shape memory. Therefore, it is also important to investigate the properties in the temperature range of the shape memory cycle.

We cut 30 mm long specimens from the dumbbell specimens to fit a 3-point bending clamp with a span of 20 mm. The test parameters were the following: a frequency of 1 Hz and an amplitude of 15 μm, in the temperature range of 30 °C–150 °C, with a heating rate of 3 °C/min.

2.3.6. Free and constrained recovery experiments

We evaluated the shape memory capabilities of the samples in both free recovery and constrained recovery cycles conducted with the same DMA device. During the experiments, the samples with a cross-section of 4 × 10 mm were cut into 30 mm long test specimens and put in a 3-point bending clamp with a 20 mm gauge length. The samples were heated to 110 °C, where they were deformed to a deflection of 2000 μm (ε_m). At

this deflection, the shape of the specimens was memorized as the samples were cooled down to 30 °C and kept there for a further 3 min. We then unloaded the specimens, measured the ε_u values from the deformation parameter of the software, and calculated R_f according to Equation (1). After shape fixation, we tested the shape recovery of the specimens. We placed them into the DMA fixture, applied a constant 0.05 N load, and heated them to 120 °C (above the deformation temperature) at a heating rate of 10 °C/min, to characterize shape memory better and ensure recovery. Then they were held at this temperature for 3 min, after which we measured ε_p from the deformation parameter of the software and calculated R_r according to Equation (2).

Besides the recovery tests mentioned above, we also performed constrained recovery cycles. Instead of a constant force, we applied a constant strain of 0.05% while the specimens were heated in this configuration to 120 °C at 10 °C/min. This time, instead of deflection, we monitored the stress the specimen exerted against the clamp during recovery, and defined σ_{rec} as the maximum of this stress.

3. Results and discussion

3.1. Flexural tests

During the 3-point bending tests, none of the samples fractured before reaching conventional deflection, indicating tough behavior. Among the various doses absorbed by the fibers, the 200 kGy (F200) samples had the highest strength (Fig. 1/a) and modulus (Fig. 1/b).

It seems that up to this dose, cross-linking took place in the material, which It seems that up to this dose, cross-linking took place in the amorphous phase, which prevented the material from melting completely at the high processing temperature. That allowed the fibers to keep their shape intact and maintain their high strength better. Above this dose (F300), cross-linking did not improve the stability of the fibers further, but it deteriorated their molecular orientation by imposing strain on the interface of the crystalline domains, decreasing their size, and disorienting the molecules (Peacock, 2000).

Unirradiated (F0) fibers could not withstand the processing temperature (200 °C) without melting. They blended with the matrix, so they did not reinforce effectively. These results corroborate the findings of our previous paper (Meszaros et al., 2022). Regarding irradiation during post-processing, doses up to 100 kGy had a minor effect on the strength or modulus of the samples. However, both the modulus and strength of the P150 and P200 samples were considerably higher, indicating that cross-linking had a major effect in this dose range. Therefore, we decided to focus on the P150 and P200 samples in our further investigation, as these are the samples that showed an enhanced shape memory effect based on the bending results.

3.2. Soxhlet extraction

We used the gel fractions [%] from Soxhlet extraction to characterize the degree of cross-linking of the samples (Table 1). With the samples not irradiated during post-processing (P0), the only potential source of the gel fraction was the fibers.

For the non-irradiated neat HDPE matrix and P0F0 reference samples, zero gel fraction was measured, indicating that both the matrix and the "blend" (including the 20 wt% fibers) were completely soluble. In the case of the samples that were not irradiated the second time, beginning with 'P0', such as P0F100, P0F200, and P0F300, we measured a gel fraction of less than 20%, indicating that these fractions came from the irradiated fibers, and so the non-irradiated HDPE matrix was dissolved. Przybytniak et al. (2008) considered around 60% gel fraction to indicate sufficient cross-linking in their study. Thus, it can be confirmed that cross-linking indeed took place in these fibers. The biggest change in gel fraction occurred between the P0F100 and P0F200 samples, with a comparatively lower change between P0F200 and P0F300. In samples irradiated twice (samples beginning with P150 and P200), the gel fractions were much higher, at around 90%, indicating that in these cases, the matrix was also cross-linked. For these two doses (150 kGy and 200 kGy) and the corresponding fiber doses, no significant changes were observed, the small differences originate from random sampling and the uncertainty inherent in the testing method.

Table 1
Gel fractions from Soxhlet extractions for different samples.

Sample	Gel fraction [%]
P0Ref	0.0
P0F0	0.0
P0F100	1.9 (9.5[a])
P0F200	8.2 (41[a])
P0F300	10.8 (54.0[a])
P150Ref	96.7
P150F0	88.8
P150F100	91.5
P150F200	92.2
P150F300	95.4
P200Ref	92.9
P200F0	97.3
P200F100	94.9
P200F200	87.4
P200F300	93.4

[a] Since the matrix was not cross-linked by irradiation, the gel fraction of the fibers was estimated (for 20 wt% fiber content).

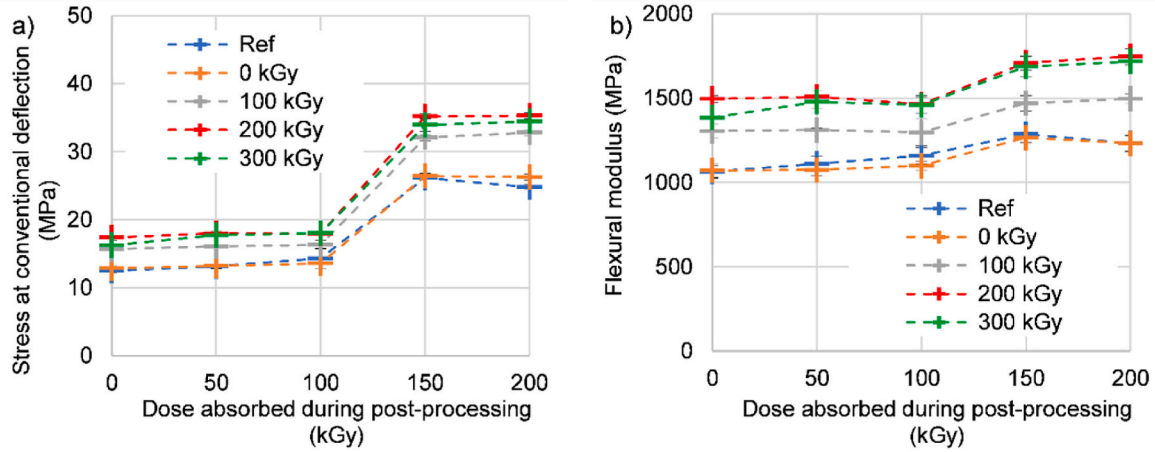

Fig. 1. a) The flexural stress at conventional deflection and b) the flexural modulus as a function of the irradiation dose absorbed during post-processing.

In conclusion, irradiation successfully cross-linked both the fiber and matrix, indicating that the fibers did indeed survive processing because of the irradiation and enabled the shape memory of the composites.

3.3. Differential scanning calorimetry (DSC)

We investigated the crystalline properties of the samples by DSC. All samples showed a single crystalline melting peak at around 130 °C, the T_m of the matrix (Fig. 2). The single melting peak indicates that the fibers recrystallized and did not retain their original crystalline structure. There were small changes in the melting enthalpies, which correspond to the degree of crystallinity. The degree of crystallinity did not change conclusively in response to irradiation during post-processing in the first heating cycle but decreased substantially in the second cycle (Table 2).

This is a well-known effect in the case of cross-linking. The cross-links inhibit the movement of the molecule segments and thus their ability to recrystallize after melting. While in the case of non-irradiated samples (beginning with P0), the degree of crystallinity in the second heating cycle was higher than in the first, in the case of the P150 and P200 samples, it was smaller. This is because some free radicals are trapped within the crystalline phase after irradiation, and these can only form new cross-links if the material is remelted. Cross-links inhibit (re) crystallization and lead to smaller crystalline domain sizes, leading to a lower T_m, as the data indicate.

Table 2
The summary of DSC.

Sample	Degree of crystallinity [%]	Crystalline melting temperature [°C]	Degree of crystallinity [%]	Crystalline melting temperature [°C]
	first heating		second heating	
P0Ref	59.3	124.2	68.2	124.3
P0F0	58.4	125.2	67.2	124.3
P0F100	60.8	125.3	63.9	123.9
P0F200	61.9	124.8	64.0	122.9
P0F300	59.2	124.0	63.0	123.5
P150Ref	59.1	121.9	57.1	120.6
P150F0	61.2	121.9	55.2	121.3
P150F100	60.7	122.1	58.9	120.6
P150F200	63.8	122.2	56.7	119.6
P150F300	57.9	122.3	54.1	121.9
P200Ref	61.8	121.4	57.8	119.2
P200F0	59.7	121.1	54.4	120.0
P200F100	58.4	121.9	55.1	120.3
P200F200	58.6	121.5	57.3	120.1
P200F300	62.2	121.2	54.3	117.2

3.4. Scanning electron microscopy (SEM)

We investigated the residues after Soxhlet extraction, specifically in the cases where only the fibers were irradiated, and so they were the only source of the gel fraction (P0F100, P0F200, and P0F300) (Fig. 3). All samples have a surface covered with micro-platelet-like structures. We think this is the effect of crystallinity, with the platelets being the crystalline lamellae after recrystallization. Fig. 3/d shows a fiber fragment, also partially recrystallized after extraction.

To confirm that the platelets shown in the images were crystalline, we performed DSC on the residues after Soxhlet extraction (Fig. 4). The DSC curves were similar to the previous DSC curves (Fig. 2).

This shows that the fibers recrystallized together with the matrix during processing. The degree of crystallinity was higher in the first heating cycle than for original samples but lower in the second heating than in the first cycle. This indicates that the solvent left a highly crystalline but also highly cross-linked structure. As a reference, we looked at samples that had parts of the matrix in the gel fraction after the Soxhlet extraction Fig. 5.

A similar, platelet-like structure can also be observed there, showing both to be the result of crystallinity. With fibers in the sample (Fig. 5/b-d), the surface was more structured and differentiated compared to P150Ref because the fibers reacted differently to the solvent (dissolved to a greater degree according to Table 1). In the case of P150F300, there were also fibers (Fig. 5/c), which recrystallized and had a different morphology than the virgin Dyneema fibers in Fig. 5/d.

3.5. Dynamic mechanical analysis (DMA)

In the DMA experiments, we focused on the T_m range, as this is the temperature range of the shape memory experiments. Therefore, we investigated the mechanical properties of the previously selected samples around the actual transition temperature as well. The storage modulus curves as a function of temperature ran parallel with each other, aside from some instabilities (Figs. 6 and 7).

The fibers and the irradiation did not affect the melting temperature. There was, however, a significant difference in the storage moduli of composites with different doses for the fibers, which reflected the flexural test results. The highest-running curves were those of the F200 and F300 samples, while the Ref samples had the lowest moduli for both doses absorbed during post-processing. The different doses adsorbed during post-processing had little effect on the storage modulus curves. The P200 samples had slightly lower storage modulus than the P150 samples, but the results with regard to the fibers were very similar.

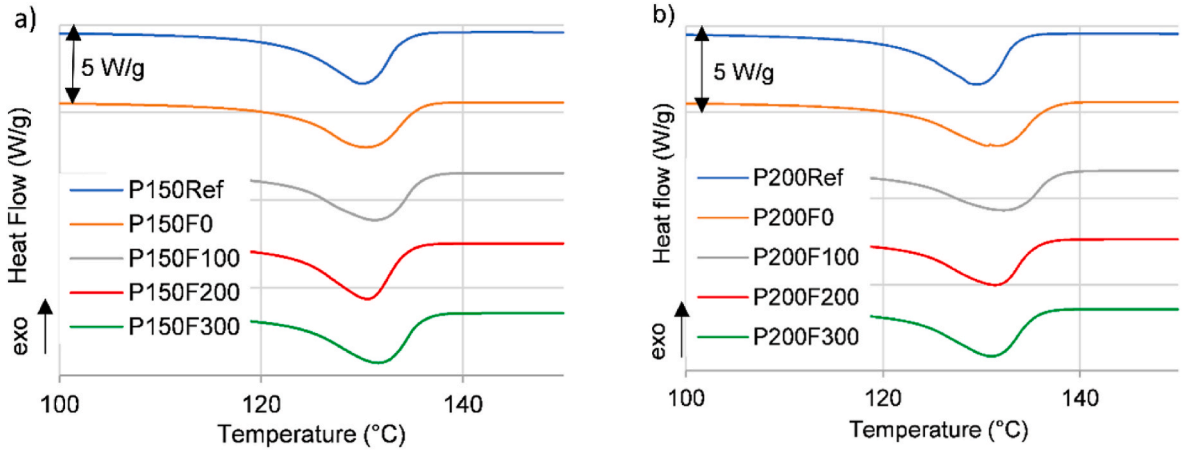

Fig. 2. DSC first heating curves for samples with an absorbed does of a) 150 kGy, and b) 200 kGy during post-processing.

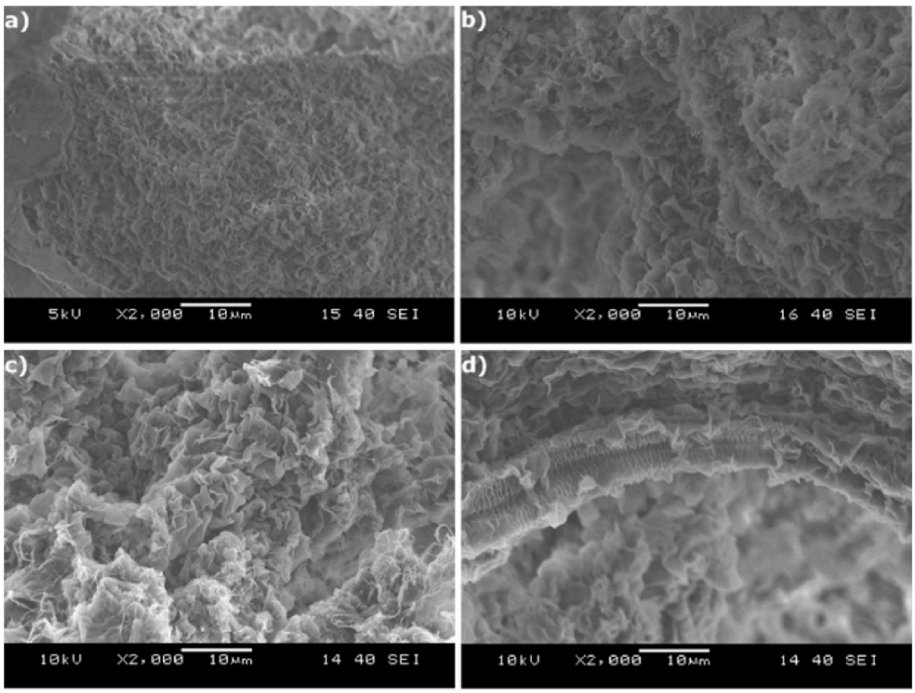

Fig. 3. SEM micrographs of the samples after the Soxhlet extractions P0F100 (a), P0F200 (b), and P0F300 (c-d).

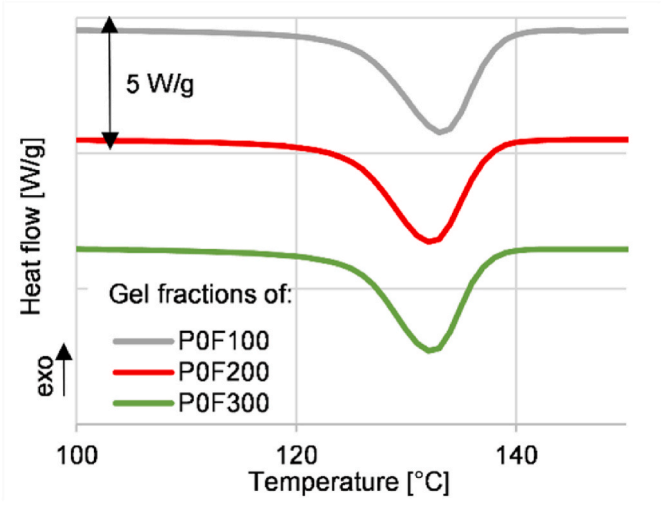

Fig. 4. First heating curves of the samples after Soxhlet extraction.

3.6. Free shape recovery experiments

The free shape recovery experiments revealed the dimensional precision of the recovery of the specimen. All the investigated samples showed good shape memory properties, with R_f and R_r above 79% (Fig. 7). The fixity ratios had no conclusive trend, likely because the ability to fix the programmed deformation depends on the crystalline domains being able to resist the internal stresses from the straining of the cross-links. Still, shape fixation improved with the addition of cross-linked fibers. Because the degrees of crystallinity and cross-link density were not greatly impacted by the fibers or the two doses (150 kGy and 200 kGy), the absorbed dose did not conclusively impact fixity. The precision of shape recovery mostly depends on the ability of the cross-links to re-deform the material to its original shape. R_r for these samples remained above 80% in all cases, with P200 samples performing better overall.

3.7. Constrained recovery experiments

In the constrained recovery experiments, all the investigated samples showed increasing stress as they were heated up to their transition temperatures, after which the stress started to decrease (Fig. 8). σ_{rec} showed good correlation with flexural strength. The F200 samples had the highest recovery stress, closely followed by the F300 samples, while the F100 and Ref samples had the lowest recovery stress.

The increase in recovery stress can be attributed to the increase in the force required to deform the samples, a part of which was then stored as internal stress by the programming and subsequently released during recovery. The σ_{rec} results of the P200 samples were slightly higher than those of the P150 samples. It is likely a result of a slightly more cross-linked structure, although the difference was smaller than the effect of the dose absorbed by the fibers.

Summarizing shape memory properties, we can clearly state that the addition of irradiated fibers to the matrix increased their recovery stress. The effect was greatest for the F200 samples. The trend in the precision of recovery was less clear. The addition of irradiated fibers, especially the F200 fibers, slightly increased the fixity ratio while slightly decreasing the recovery ratio. All samples still retained a sufficiently precise shape memory behavior.

4. Demonstration

We demonstrated the shape memory of the specimen by making a small propeller system from the P200F200 sample, as it performed the best in the tests. We machined two bearing housings out of a tensile specimen. The material was notably well-suited to machining. Then, we heated up the bearing housing with a blowtorch, opened it to create the programmed shape, and let it cool down. Placing the bearing in the housing, we heated it up again to cause the housing to close tightly around the bearing (Fig. 9).

We then tested shape memory on the propeller. We assembled the two bearing housings and the axle and put the propeller on the end. We heated up and deformed the propeller in the same way, then let it cool down to lock the programmed shape (Fig. 10). We heated it up again, and it recovered its shape. As recovery is not 100% precise, a more

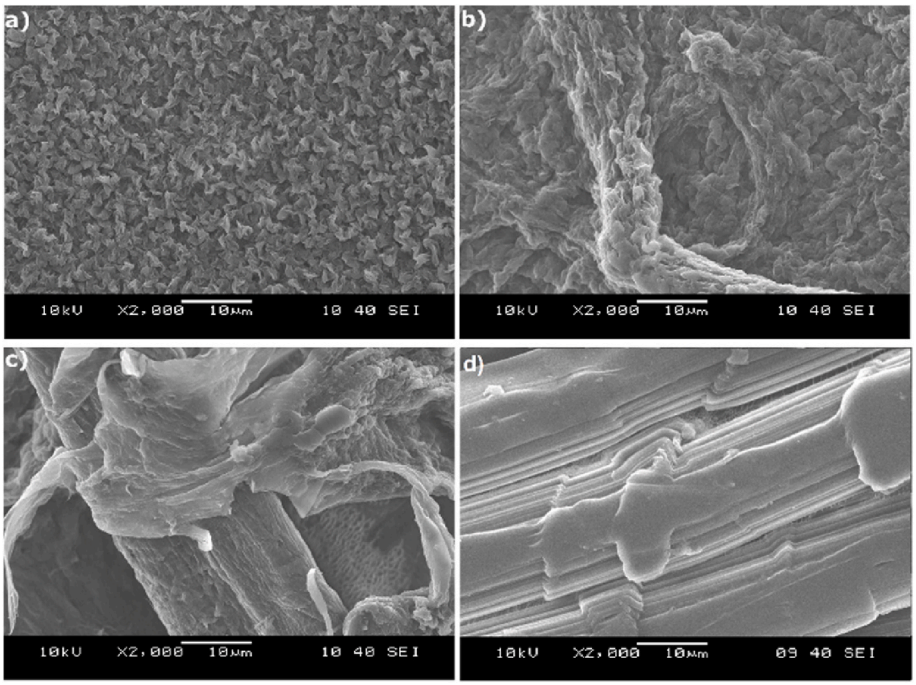

Fig. 5. SEM micrographs of the samples after Soxhlet extraction. a) HDPE matrix with no fibers, irradiated with 150 kGy (P150Ref), b)-c) P150F300 sample, and d) virgin Dyneema fibers.

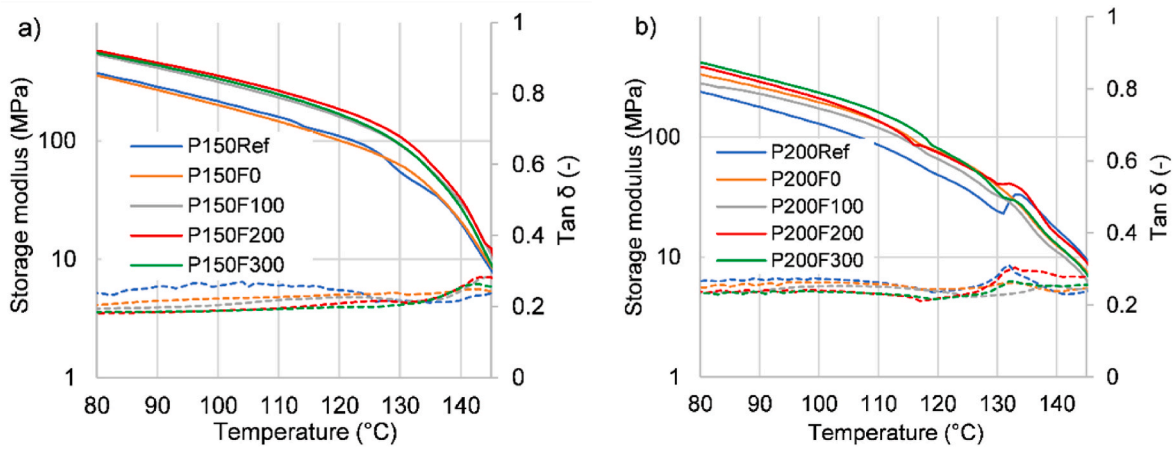

Fig. 6. Storage modulus curves of a) P150 samples and b) P200 samples.

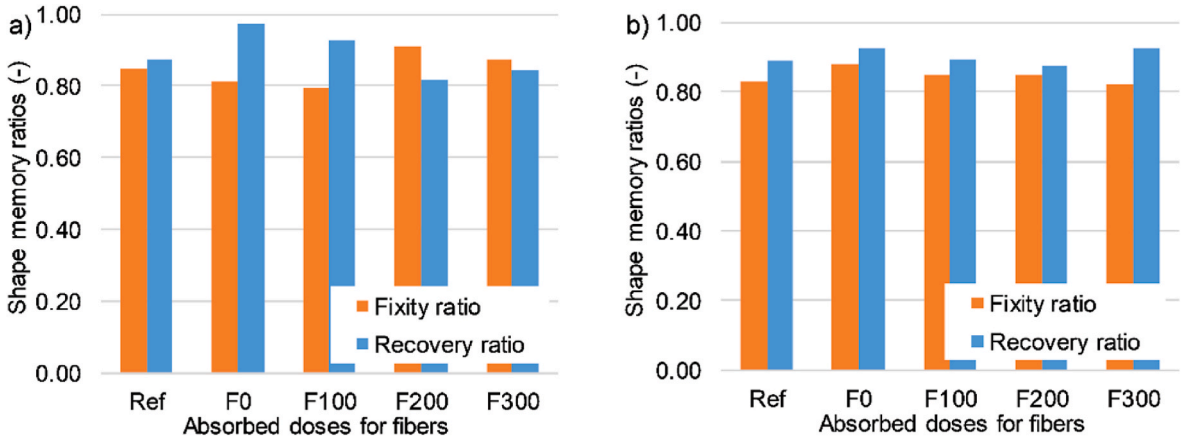

Fig. 7. Recovery and fixity ratios of a) P150 and b) P200 samples.

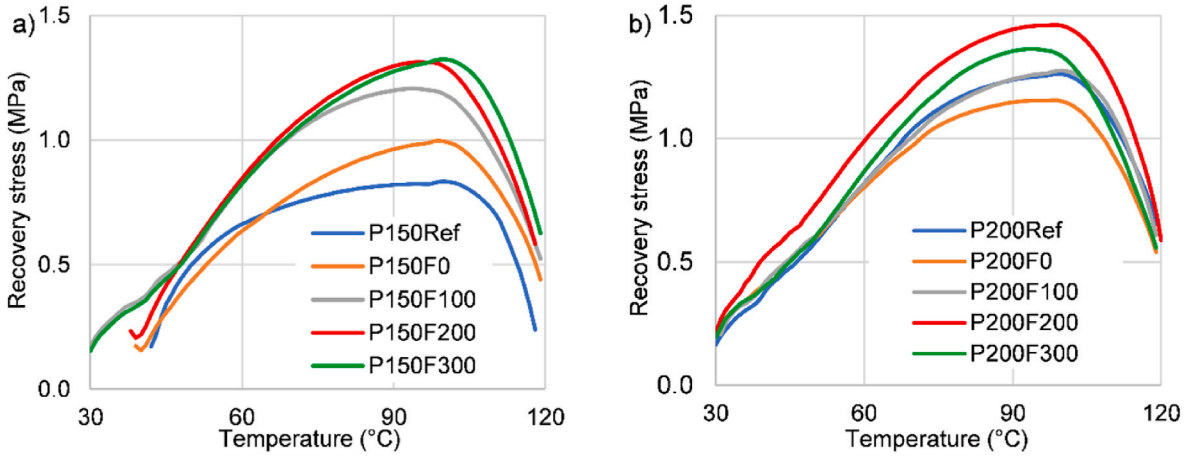

Fig. 8. Recovery stress curves of the a) P150 b) P200 samples.

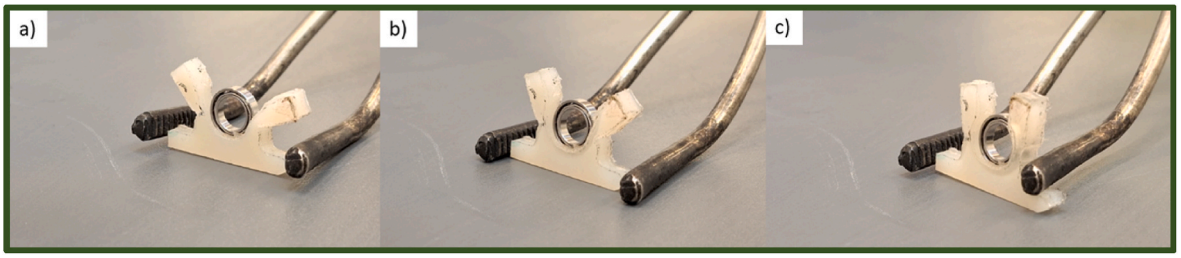

Fig. 9. Demonstration of shape memory on a bearing housing. Programmed shape (a), recovery process (b), and recovered shape (c).

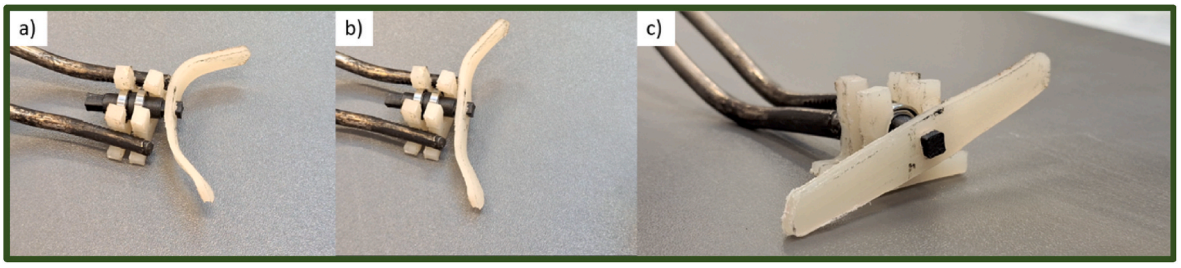

Fig. 10. Demonstration of shape memory on a propeller. Programmed shape (a), recovery process (b) and recovered shape (c).

deformed geometry has to be produced by machining than the exact geometry we want to recover.

5. Conclusions

In this study, we evaluated the effects of a novel self-reinforcing method on the shape memory properties of X-PE. In this method, we employed two steps of irradiation, one on the fibers to enable them to withstand processing and one during post-processing to enable shape memory. We found that the irradiated self-reinforced composites had good mechanical and shape memory properties. In mechanical tests, we found that maximum strength and modulus were achieved when fibers were irradiated with a dose of 200 kGy beforehand. These fibers withstood injection molding best. Soxhlet extraction, DSC experiments, and SEM micrographs confirmed cross-linking in both fibers and composites and that fibers survived processing at 200 °C. They also showed that the fibers recrystallized during processing.

All irradiated self-reinforced composites showed good shape memory properties in both constrained and free recovery experiments, with R_r and R_f above 79% in all cases. Recovery stress correlated with the strength of the composite, and the F200 samples performed best. The experiments proved the viability of self-reinforcement and its ability to improve the shape memory characteristics of X-PE; the best composite regarding shape memory properties had fibers irradiated with 200 kGy and was irradiated after processing with 200 kGy. In this case, recovery stress increased by 26%, while the precision of recovery was barely affected; the recovery ratio decreased by 1% and the fixity ratio increased by 2%.

CRediT authorship contribution statement

Balázs Tatár: Writing – original draft, Visualization, Validation, Investigation. **Eszter Tóth:** Validation, Investigation. **Kolos Molnár:** Writing – review & editing, Validation, Supervision, Methodology, Conceptualization. **László Mészáros:** Writing – review & editing, Writing – original draft, Supervision, Resources, Funding acquisition, Conceptualization.

Declaration of competing interest

The authors declare that they have no known competing financial interests or personal relationships that could have appeared to influence

the work reported in this paper.

Acknowledgments

This work was supported by the National Research, Development and Innovation Office, Hungary (FK138501). Project no. TKP-6-6/PALY-2021 has been implemented with the support provided by the Ministry of Culture and Innovation of Hungary from the National Research, Development and Innovation Fund, financed under the TKP2021-NVA funding scheme.The authors also extend their acknowledgment to the International Atomic Energy Agency (IAEA) for financial support under the umbrella of CRP (Coordinated Research Project). László Mészáros and Kolos Molnár are thankful for the János Bolyai Research Scholarship of the Hungarian Academy of Sciences, and László Mészáros was supported by the ÚNKP-23-5-BME-434 New National Excellence Program of the Ministry for Culture and Innovation from the source of the National Research, Development and Innovation Fund.

Data availability

Data will be made available on request.

References

Amer, M.S., Ganapathiraju, S., 2001. Effects of processing parameters on axial stiffness of self-reinforced polyethylene composites. J. Appl. Polym. Sci. 81 (5), 1136–1141.
Behl, M., Zotzmann, J., Lendlein, A., 2010. Shape-Memory Polymers. Springer, Berlin, Heidelberg, Germany.
Bhanushali, H., Amrutkar, S., Mestry, S., Mhaske, S.T., 2022. Shape memory polymer nanocomposite: a review on structure-property relationship. Polym. Bull. 79 (6), 3437–3493.
Fejos, M., Romhany, G., Karger-Kocsis, J., 2012. Shape memory characteristics of woven glass fibre fabric reinforced epoxy composite in flexure. J. Reinforc. Plast. Compos. 31 (22), 1532–1537.
Hine, P.J., Ward, I.M., El Matty, M.I.A., Olley, R.H., Bassett, D.C., 2000. The hot compaction of 2-dimensional woven melt spun high modulus polyethylene fibres. J. Mater. Sci. 35 (20), 5091–5099.
Hine, P.J., Ey, R.H., Ward, I.M., 2008. The use of interleaved films for optimising the production and properties of hot compacted, self reinforced polymer composites. Compos. Sci. Technol. 68 (6), 1413–1421.
Huang, Y.-F., Xu, J.-Z., Xu, J.-Y., Zhang, Z.-C., Hsiao, B.S., Xu, L., Li, Z.-M., 2014a. Self-reinforced polyethylene blend for artificial joint application. J. Mater. Chem. B 2 (8), 971–980.
Huang, Y.-F., Xu, J.-Z., Li, J.-S., He, B.-X., Xu, L., Li, Z.-M., 2014b. Mechanical properties and biocompatibility of melt processed, self-reinforced ultrahigh molecular weight polyethylene. Biomaterials 35 (25), 6687–6697.
Jeewantha, L.H.J., Epaarachchi, J.A., Forster, E., Islam, M., Leng, J., 2022. Early research of shape memory polymer vascular stents. Express Polym. Lett. 16, 902–923.
Jyotishkumar, P., Suchart, S., Jinu, J.G., Seno, J., Shape Memory Polymers, 2019. Blends and Composites Advances and Applications. Springer, Singapore.
Kara, Y., Molnar, K., 2022. Melt-blown fiber mat interleaving enhances the performance of single-polypropylene composites. J. Reinforc. Plast. Compos. 41 (23–24), 963–974.
Kmetty, A., Barany, T., Karger-Kocsis, J., 2010. Self-reinforced polymeric materials: a review. Prog. Polym. Sci. 35 (10), 1288–1310.
Kmetty, A., Barany, T., Karger-Kocsis, J., 2012. Injection moulded all-polypropylene composites composed of polypropylene fibre and polypropylene based thermoplastic elastomer. Compos. Sci. Technol. 73, 72–80.
Kmetty, A., Tabi, T., Kovacs, J.G., Barany, T., 2013. Development and characterisation of injection moulded, all-polypropylene composites. Express Polym. Lett. 7 (2), 134–145.
Li, F.F., Scarpa, F., Lan, X., Liu, L.W., Liu, Y.J., Leng, J.S., 2019. Bending shape recovery of unidirectional carbon fiber reinforced epoxy-based shape memory polymer composites. Compos. Appl. Sci. Manuf. 116, 169–179.
Li, Y., Min, L., Xin, J.H., Wang, L.H., Wu, Q.H., Fan, L.F., Gan, F., Yu, H., 2022. High-performance fibrous artificial muscle based on reversible shape memory UHMWPE. Journal of Materials Research and Technology-Jmr&T 20, 7–17.
Liu, Y.F., Wu, J.L., Song, S.L., Xu, L.X., Chen, J., Peng, W., 2018. Thermo-mechanical properties of glass fiber reinforced shape memory polyurethane for orthodontic application. J. Mater. Sci. Mater. Med. 29 (9), 148.
Maksimkin, A., Kaloshkin, S., Zadorozhnyy, M.V., Tcherdyntsev, V., 2014. Comparison of shape memory effect in UHMWPE for bulk and fiber state. J. Alloys Compd. 586, S214–S217.
Maksimkin, A.V., Kaloshkin, S.D., Zadorozhnyy, M.V., Senatov, F.S., Salimon, A.I., Dayyoub, T., 2018. Artificial muscles based on coiled UHMWPE fibers with shape memory effect. Express Polym. Lett. 12 (12), 1072–1080.
Maksimkin, A.V., Larin, I.I., Chukov, D.I., Zadorozhnyy, M.Y., Dayyoub, T., Zadorozhnyy, V.Y., Spieckermann, F., Soprunyuk, V., 2019. Coiled artificial muscles based on UHMWPE with large muscle stroke. Mater. Today Commun. 21.
Mészáros, L., Tatár, B., Toth, K., Földes, A., Nagy, K.S., Jedlovszky-Hajdu, A., Tóth, T., Molnár, K., 2022. Novel, injection molded all-polyethylene composites for potential biomedical implant applications. J. Mater. Res. Technol. 17, 743–755.
Meszaros, L., Tatar, B., Toth, K., Foldes, A., Nagy, K.S., Jedlovszky-Hajdu, A., Toth, T., Molnar, K., 2022. Novel, injection molded all-polyethylene composites for potential biomedical implant applications. Journal of Materials Research and Technology-Jmr&T 17, 743–755.
Nemes-Károly, I., Szebényi, G., 2023. Improving optical damage analysis of knee implants from an engineering perspective. Period. Polytech. - Mech. Eng. 67 (2), 151–160.
Ota, S., 1981. Current status of irradiated heat-shrinkable tubing in Japan. Radiat. Phys. Chem. 18 (1–2), 81–87.
Peacock, A.J., 2000. Handbook of Polyethylene : Structures, Properties, and Applications. Dekker, New York.
Przybytniak, G., Nowicki, A., Mirkowski, K., 2008. Evaluation of polymers designed for radiation processing. Nukleonika 53, S67–S72.
Rahman, A.A., Ikeda, T., Senba, A., 2017. Memory effects performance of polyurethane shape memory polymer composites (SMPC) in the variation of fiber volume fractions. Fibers Polym. 18 (5), 979–986.
Rezanejad, S., Kokabi, M., 2007. Shape memory and mechanical properties of cross-linked polyethylene/clay nanocomposites. Eur. Polym. J. 43 (7), 2856–2865.
Tatár, B., Mészáros, L., 2024. Shape memory effect in cross-linked polyethylene matrix composites: the effect of the type of reinforcing fiber. Polym. Bull. 81 (7), 6311–6323.
Vadas, D., Kmetty, A., Barany, T., Marosi, G., Bocz, K., 2018. Flame retarded self-reinforced polypropylene composites prepared by injection moulding. Polym. Adv. Technol. 29 (1), 433–441.
Wang, Y.K., Zhu, G.M., Tang, Y.S., Liu, T.T., Xie, J.Q., Ren, F., 2014a. Short glass fiber reinforced radiation crosslinked shape memory SBS/LLDPE blends. J. Appl. Polym. Sci. 131 (17), 40691.
Wang, Y.K., Zhu, G.M., Xie, J.Q., Men, Q.N., Liu, T.T., Ren, F., 2014b. An investigation on shape memory behavior of glass fiber/SBS/LDPE composites. J. Polym. Res. 21 (8), 515.
Wang, Y.K., Tian, W.C., Zhu, G.M., Xie, J.Q., 2016. Thermomechanical and shape memory properties of SCF/SBS/LLDPE composites. Chin. J. Polym. Sci. 34 (11), 1354–1362.
Wang, J., Wang, D., Mao, Q., Chen, J., 2022. Fabric insert injection molding for the preparation of ultra-high molecular weight polyethylene/high-density polyethylene two-component self-reinforced composites. Polymers 14 (20).
Wunderlich, B., 2012. Thermal Analysis. Academic Press, San Diego.
Xia, Y.L., He, Y., Zhang, F.H., Liu, Y.J., Leng, J.S., 2021. A review of shape memory polymers and composites: mechanisms, materials, and applications. Adv. Mater. 33.
Zhang, M.Q., 2022. Shape memory polymer capable of gradual transformation and working. Express Polym. Lett. 16 (10), 1011-1011.
Zhang, Y., Müller, M.T., Boldt, R., Stommel, M., 2023. Crystallinity effect on electron-induced molecular structure transformations in additive-free PLA. Polymer 265, 125609.